Chapter 5
Robustness of Orthogonal Eigenstructure Control to Actuators Failure

Mohammad Rastgaar and Nina Mahmoudian

Abstract Orthogonal eigenstructure control (OEC) is a feedback control method applicable to multi-input multi-output linear systems. While the available control design methodologies offer a large and complex design space of options that can often overwhelm a designer, this control method offers a significant simplification of the design task while still allowing some experience-based design freedom. In this chapter, the robustness of the method to the failure of the actuators was investigated. It was shown the control gain was capable of controlling the systems during an actuator failure, as OEC generates the control gain by maintaining the closed-loop eigenvectors within the achievable eigenvectors set. A system of lumped masses was used to explain the method; then, the problem of failed actuators in the vibration control of a plate was investigated. Finite element analysis was used for modeling the plate to simulate the dynamic behavior of the system. Five cases were considered and the suppression of the vibration in a plate with three working actuators was compared to the performance of a similar control system with a failed actuator. Also, the behaviors of the system with failed actuators were compared to the systems that were designed to operate with lesser control actuators. It was shown that the number of closed-loop eigenvalue pairs that moved from the cluster of the open-loop poles was equal to the number of working actuators. The closed-loop poles in all the systems were moved to the vicinity of one specific area, generating a break frequency with sufficient damping for robust active vibration control.

M. Rastgaar (✉) • N. Mahmoudian
Mechanical Engineering–Engineering Mechanics Department, Michigan Technological University, Houghton, MI 49931, USA
e-mail: rastgaar@mtu.edu

R.N. Jazar and L. Dai (eds.), *Nonlinear Approaches in Engineering Applications 2*,
DOI 10.1007/978-1-4614-6877-6_5,

5.1 Introduction

OEC was developed to address the need for more robust control method that is relatively easy to design and implement and allows control engineers to achieve good performing designs even with little design experience. In this chapter, the problem of robustness of the vibration control to the failure of actuators was investigated using OEC, a feedback control method applicable to multi-input multi-output linear systems. While the available control design methodologies offer a large and complex design space of options that can often overwhelm a designer, this control method offers a significant simplification of the design task while still allowing some experience-based design freedom. This control method needs neither predefining the locations for the closed-loop poles nor shaping the closed-loop eigenvectors. The orthogonal eigenstructure control regenerates the open-loop system and simultaneously finds the vectors that are orthogonal to its eigenvectors. The determined orthogonal vectors are within the achievable eigenvectors set, so the error due to the difference between achievable eigenvectors and the desirable eigenvectors, as is common in eigenstructure assignment methods, is eliminated. It has been shown that eigenstructure assignment methods are effective for active vibration cancelation in structures. The methods currently available, however, depend on the experience of the controller designer, based on the geometry and dynamics of the structures. In general, there are no unified methods for the application of eigenstructure assignment with the purpose of vibration cancelation in structures. Existing methods require *apriori* definition of the desired eigenstructure [1]. Identifying the desirable locations for the closed-loop eigenvalues and defining the desirable closed-loop eigenvectors are not a straightforward task [2]. For large scale systems it becomes impractical to define a desired closed-loop eigenstructure. Therefore, the existing methods are not able to be applied to such systems or many other similar practical engineering structures. Considering that there are no one-to-one relationship between the elements of closed-loop eigenvectors and the states of the system, one may define a desirable eigenvector, but not achievable, that does not satisfy a given design criterion. This may lead to excessive actuation forces because of improper closed-loop poles. Additionally, the desirable eigenvectors do not necessarily lie within the space of achievable eigenvectors. The missing piece of this puzzle is a control method that can systematically lead to a set of desirable, and obviously achievable, closed-loop eigenvectors that result in a decoupled control and less sensitive to actuator failure.

Critical issues may arise when the actuator fails in a system. The application of robustness of control methods to actuator failure by absorbing some of the impacts on the performance of the control system may prevent a complete failure of the system and allow for delayed maintenance. Many researchers have investigated different methods to accommodate actuator failure in a variety of applications. A method for actuator failure was proposed by Tao et al. as a direct adaptive state feedback control scheme for linear time-invariant systems [3–5]. Their method was model based and the failure pattern was simulated such that some of the control

inputs were stuck at unknown values at unknown time instants. They investigated the conditions and controller structures for matching system and model states during actuator failure. Tang et al. proposed a method with a similar concept for multi-input multi-output nonlinear systems [6]. Fei et al. developed an output feedback control for output tracking in discrete linear time-invariant systems, with uncertain failures [7]. Some methods address the failure of actuators by multiple model design, for example, Chen et al. studied the problem of actuator failure for linear and nonlinear systems [8]. In this method, all the possible scenarios of the actuator failure were accumulated and used for both state and output feedback control by combining the observer design with the adaptation method. Also, a design technique to prevent stuck actuators was proposed by Chen et al. based on an iterative learning observer and designing a reconfigurable controller using estimated states to compensate for the effect of the failed actuators [9]. The optimal control approach was also used for compensating the effect of failed actuators. Yang et al. studied a low-cost LQ regulator for discrete-time systems with actuator failure [10]. Seo et al. considered the actuator failures as disturbance signals of arbitrary values to the system, and designed a robust and reliable H_∞ state feedback control for linear uncertain systems with time-varying norm-bounded parameter uncertainty [11]. Wang et al. proposed a H_∞ control for a class of switched nonlinear systems with actuator failures among a prespecified subset of the situations of the actuators' failure [12]. They used a multiple-Lyapunov function method to derive a sufficient condition for the switched nonlinear system to be asymptotically stable with H_∞ norm bound. Zhao et al. used a linear Matrix Inequality Approach (LMI) for state feedback control design applied to a class of systems with model uncertainties and actuators' failures [13].

The eigenstructure assignment methods have been used to address the problem of actuator failure and reconfiguring the systems. Liu et al. combined the time-domain performance specifications provided by eigenstructure assignment and robust performance specifications in the frequency domain considered by H_∞ control to develop a joint optimal robust control design [14]. A method for designing the reconfiguring class of second-order systems has been proposed by Wang et al. based on the parametric eigenstructure assignment by PD feedback developed earlier by Duan [15]. This method finds the parametric forms of all the re-synthesized gain matrices. Zhang et al. proposed an integrated fault detection, diagnosis, and reconfigurable control scheme based on the interacting multiple model approach and used an eigenstructure assignment technique for reconfigurable feedback control law design [16]. Another method based on the eigenstructure assignment method for reconfiguring the control system to recover the eigenvalues and eigenvectors of the original closed-loop system has been presented by Jiang et al. [17]. This method leads to a stable system when full state feedback is available and, for the output feedback problems, recovers the subsequent dominant eigenvalues and eigenvectors of the original system. Apkarian et al. used the eigenstructure assignment with Lyapunov-type constraints to develop a control method with enhanced LMI characterizations [18].

OEC was introduced by the authors [19] and was developed further for systems with non-collocated actuators and sensors [20]. Application of OEC in high degrees of freedom systems was presented in [21]. The experimental application of this method for active vibration cancelation using piezoelectric actuators was shown in [22]. A comparison of OEC with eigenstructure assignment techniques was discussed in [23].

In this chapter we evaluated the robustness of OEC when used for vibration cancelation in a plate. First, we defined the orthogonal eigenstructure control. Then, using a simple lumped mass model, we described how the method provided the control gain matrix such that both the closed-loop system with working actuators and the one with the failed actuator have eigenvectors within achievable eigenvectors set. Finally, we applied the control method to a finite element model of a plate and investigated the vibration cancelation in the presence of the failed actuator. Comparisons were made between systems with three working actuators and systems with two working and one failed actuators. Moreover, a comparison between the systems with two working and one failed actuators were compared to the systems that were designed specifically with two actuators.

5.2 Orthogonal Eigenstructure Control

Let's consider the first order realization of a closed-loop multi-input multi-output linear system;

$$\dot{x} = Ax + Bu + Ef \tag{5.1}$$

$$y = Cx \tag{5.2}$$

$$u = Ky \tag{5.3}$$

where x and $\dot{x}$ are the $2n \times 1$ state vector and its time derivative, A is the $2n \times 2n$ state matrix, B is a $2n \times m$ input matrix, where $m \geq 2$ is the number of the actuators, E is the disturbance input matrix, f is the disturbance vector with appropriate dimensions, and u is the input vector of dimension m. Assume the actuators and sensors are colocated; therefore, the output vector y is $m \times 1$ and the output matrix C is $m \times 2n$. K is $m \times m$ feedback gain matrix. The closed-loop equation of motion is

$$\dot{x} = (A + BKC)x + Ef \tag{5.4}$$

For the closed loop system of Eq. (5.4), the eigenvalue problem is defined as

$$(A + BKC)\phi_i = \lambda_i \phi_i \quad i = 1, \ldots, 2n \tag{5.5}$$

where ϕ_i and λ_i are the closed-loop eigenvectors and eigenvalues of the system, respectively. Equation (5.5) may be written in matrix form as follows:

$$[A - \lambda_i I \ | B] \begin{Bmatrix} \phi_i \\ KC\phi_i \end{Bmatrix} = 0 \ i = 1, \ldots, 2n \tag{5.6}$$

where I is the $2n \times 2n$ identity matrix. Equation (5.6) implies that the vector $\begin{Bmatrix} \phi_i \\ KC\phi_i \end{Bmatrix}$ spans the null space of the matrix $S_{\lambda i} = [A - \lambda_i I \ | B]_{2n \times (2n+m)}$. Calculating the singular value decomposition of $S_{\lambda i}$, we may write

$$S_{\lambda i} = [U_i]_{2n \times 2n} [\Sigma_i | 0_{2n \times m}]_{2n \times (2n+m)} [V_i^*]_{(2n+m) \times (2n+m)} \tag{5.7}$$

U_i and V_i are the left and right orthonormal matrices, respectively, and V_i^* is the conjugate transpose of the complex matrix V_i. The index i specifies the equations for the ith operating eigenvalue. In OEC, operating eigenvalue λ_i are chosen from the open-loop eigenvalues set. Substituting operating eigenvalue λ_i in Eq. (5.6) allows for regenerating the open-loop system and systems with eigenvectors almost orthogonal to the eigenvectors of the regenerated open-loop system simultaneously. The number of operating eigenvalues is the same as the number of the required pairs of actuators and sensors m. It has been shown that the m farthest open-loop eigenvalues from the origin are proper options for the operating eigenvalues [21]. After partitioning V_i, the second column block of V_i spans the null space of $S_{\lambda i}$ [24, 25].

$$[V_i]_{(2n+m) \times (2n+m)} = \begin{bmatrix} [V_{11}^i]_{2n \times 2n} & [V_{12}^i]_{2n \times m} \\ [V_{21}^i]_{m \times 2n} & [V_{22}^i]_{m \times m} \end{bmatrix} \tag{5.8}$$

An achievable eigenvector ϕ_i^a of the closed-loop system is any linear combination of m columns of V_{12}^i using a coefficient vector r^i.

$$\phi_i^a = V_{12}^i r^i \tag{5.9}$$

The control gain matrix K is defined as

$$KC\phi_i^a = V_{22}^i r^i \tag{5.10}$$

which requires finding the appropriate r^i. We define the modal energy corresponding to the ith achievable eigenvector of the closed-loop system:

$$E_i = r^{i*} V^* V_{12}^i r^i \tag{5.11}$$

Since V_{12}^i is complex, then ${V_{12}^i}^* V_{12}^i$ is a Hermitian matrix and its eigenvalue decomposition is

$$V_{12}^{i}{}^{*}V_{12}^{i} = \bar{U}^{i}\Lambda^{i}\bar{U}^{i*} \tag{5.12}$$

where $\bar{\Lambda}_i$ and $\bar{U}^i$ are the eigenvalues and eigenvectors matrices of $V_{12}^{i}{}^{*}V_{12}^{i}$. Similarly, V_{22}^{i} is a complex matrix and the eigenvalue decomposition of the Hermitian matrix $V_{22}^{i}{}^{*}V_{22}^{i}$ is

$$V_{22}^{i}{}^{*}V_{22}^{i} = \bar{U}_{w}^{i}\bar{\Lambda}_{w}^{i}\bar{U}_{w}^{i*} \tag{5.13}$$

where $\bar{\Lambda}_{w}^{i}$ and $\bar{U}_{w}^{i}$ are the eigenvalue and eigenvector matrices of $V_{22}^{i}{}^{*}V_{22}^{i}$. It has been shown by the authors [24, 26] that the eigenvalues of the Hermitian products $V_{12}^{i}{}^{*}V_{12}^{i}$ and $V_{22}^{i}{}^{*}V_{22}^{i}$ belong to the [0 1] interval. Moreover, it has been shown that the eigenvectors of $V_{22}^{i}{}^{*}V_{22}^{i}$ and $V_{12}^{i}{}^{*}V_{12}^{i}$ are identical and the summation of the eigenvalues of $V_{12}^{i}{}^{*}V_{12}^{i}$ and $V_{22}^{i}{}^{*}V_{22}^{i}$ associated with similar eigenvectors are in unity [24, 26].

$$\bar{\Lambda}_{w}^{i} + \bar{\Lambda}^{i} = I \tag{5.14}$$

$$\bar{U}^{i} = \bar{U}_{w}^{i} \tag{5.15}$$

Rearranging the Eq. (5.12) implies

$$\bar{U}^{i*}V_{12}^{i}{}^{*}V_{12}^{i}\bar{U}^{i} = \bar{\Lambda}^{i} \tag{5.16}$$

If the eigenvector $\bar{U}_J^i$ associated with a unity eigenvalue of $V_{12}^{i}{}^{*}V_{12}^{i}$ in Eq. (5.11) is considered as r^i, its modal energy $E^i = 1$.

$$\bar{U}_J^{i*}V_{12}^{i}{}^{*}V_{12}^{i}\bar{U}_J^{i} = 1 \tag{5.17}$$

That results in

$$\bar{U}_J^{i*}(V_{22}^{i}{}^{*}V_{22}^{i})\bar{U}_J^{i} = 0 \tag{5.18}$$

Equations (5.17) and (5.18) yield

$$V_{22}^{i}\bar{U}_J^{i} = 0 \tag{5.19}$$

which results in the zero gain matrix

$$KC\phi_i^a = V_{22}^{i}r^i = V_{22}^{i}\bar{U}_J^{i} = 0 \tag{5.20}$$

which implies that the open-loop system has been regenerated. Therefore, if the eigenvector $\bar{U}_J^i$ associated with a unity eigenvalue of $V_{12}^{i}{}^{*}V_{12}^{i}$ is selected as r^i, one can generate the open-loop eigenvectors within the null space of the closed-loop eigenvectors associated with the operating eigenvalue λ_i. In other words, $V_{12}^{i}\bar{U}_J^{i}$

is parallel to the eigenvector corresponding to the open-loop eigenvalue or the operating eigenvalue. Any other eigenvectors associated with non-unity eigenvalues of ${V_{12}^i}^* V_{12}^i$ are orthogonal to the eigenvector associated with the unity eigenvalue of ${V_{12}^i}^* V_{12}^i$. Therefore, a set of closed-loop eigenvectors can be found that are orthogonal to the open-loop ones. The modal energies associated with the closed-loop eigenvectors are equal to non-unity eigenvalues of ${V_{12}^i}^* V_{12}^i$. Since all the non-unity eigenvalues of ${V_{12}^i}^* V_{12}^i$ are small, the modal energies of the modes associated with the operating eigenvalues become zero or negligible.

V and W are determined by appending the calculated closed-loop eigenvectors for all the operating eigenvalues

$$V = \left[V_{12}^1 r^1 \cdots V_{12}^m r^m\right] \tag{5.21}$$

$$W = \left[V_{22}^1 r^1 \cdots V_{22}^m r^m\right] \tag{5.22}$$

The control gain matrix K is

$$K = W(CV)^{-1} \tag{5.23}$$

The state matrix of the closed-loop system is

$$A_c = A + BKC \tag{5.24}$$

There are m eigenvectors belong to ${V_{12}^i}^* V_{12}^i$ that can be chosen as r^i. Therefore, there are m^m possible closed-loop systems. ${V_{12}^i}^* V_{12}^i$ has one unity eigenvalue and $m-1$ zero or negligible ones. Excluding the regenerated open-loop system, there are $m^m - 1$ possible closed-loop systems.

Most of the eigenstructure assignment methods use a different approach such as eigenvector shaping to define a desired eigenvector for the system [ϕ_i^a in Eq. (5.10)]. In general, methods that use the pseudo inverse of V_{12}^i to find the required r^i have limitations because there is always a distance between the desired and controlled eigenvectors and the controlled eigenvectors will not be identical to the desired ones. This is not an issue in OEC.

Figure 5.1 shows the open-loop eigenvectors and achievable closed-loop eigenvectors of a system with three collocated actuators and sensors. For each open-loop eigenvector associated with one operating eigenvalue, two orthogonal eigenvectors can be found within the achievable eigenvectors set. To have a closed-loop system, it is sufficient to alter just one open-loop eigenvector and replace it with an orthogonal vector. It results in $3^3 - 1 = 26$ closed-loop systems from which the most desirable one must be chosen. It has been shown, however, that for a high dimensional system like a plate, if the operating eigenvalues are chosen as the farthest open-loop eigenvalues from the origin, all the possible closed-loop system converge [21].

In the next sections, we used the OEC to isolate the vibrations due to the disturbance in the system with lumped masses. We explained how the failure of one actuator does not change the behavior of the system, since the reduced gain matrix still was able to generate a closed-loop system with eigenvalues close those of the

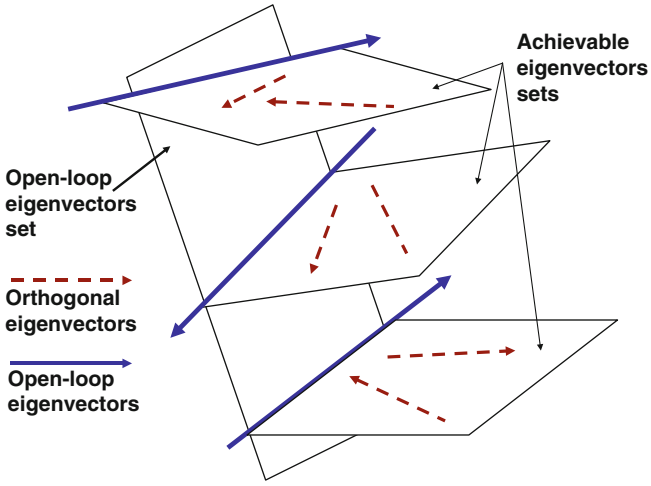

Fig. 5.1 Schematics of the process of orthogonal eigenstructure control. Open-loop eigenvectors are the intersections of the open-loop eigenvectors set and the achievable eigenvectors set. The orthogonal eigenvectors within the achievable eigenvectors set are being substituted as the open-loop ones

system with working actuators. Also, it was shown that the closed-loop eigenvectors were within the achievable eigenvectors set. Then, the OEC was applied to a plate for vibration suppression, and the robustness of the control to the failure of the actuators was investigated.

5.3 Explanatory Example: System of Lumped Masses

To investigate the effects of failure of one of the actuators during the control of a system, a simple system of longitudinally vibrating masses was considered. First, we applied OEC to isolate the left side of the system from vibrating. As shown on Fig. 5.2, the system consisted of 10 masses which were consecutively connected by springs and dampers. The force disturbance was considered to be a chirp input applied to m_{10}. It reached from 0 Hz to 30 Hz in 1 s with magnitude of 500 N. All masses were 100 kg, and damping coefficients were assumed to be 10 N s m^{-1}. The stiffnesses of the springs were 2,000 N m^{-1}.

We assumed there were three pairs of collocated actuators and sensors on masses m_6, m_7, and m_8. For simplicity, all the elements of the B and C matrices were assumed to be zero except for

$$B(16,1) = B(17,2) = B(18,3) = -1/100$$
$$C(1,6) = C(2,7) = C(3,8) = 1$$

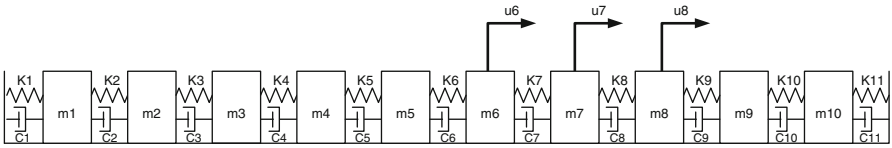

Fig. 5.2 Actuation forces for the system with failed actuator

As stated earlier, since there were three actuators and sensors, the operating eigenvalues were the three greatest open-loop eigenvalues [21]. Knowing that the complex conjugates of the operating eigenvalues lead to similar results, the operating eigenvalues were $\lambda_1 = -0.4919 + 8.8396\text{i}$, $\lambda_2 = -0.4683 + 8.5692\text{i}$, and $\lambda_3 = -0.4310 + 8.1246\text{i}$.

Following the procedure of the OEC, for the first operating eigenvalue λ_1, the product of the complex conjugate of the basis of the null space to the matrix itself could be written as follows:

$$V_{12}^{1*}V_{12}^{1} = \begin{bmatrix} 0.4128 & -0.3789 & 0.3143 \\ -0.3789 & 0.3479 & -0.2886 \\ 0.3143 & -0.2886 & 0.2394 \end{bmatrix} = \bar{U}^1\bar{\Lambda}^1\bar{U}^{1*}$$

$$= \underbrace{\begin{bmatrix} -0.6425 & -0.6699 & 0.3722 \\ 0.5898 & -0.1222 & 0.7982 \\ -0.4892 & 0.7324 & 0.4736 \end{bmatrix}}_{\bar{U}_1^1 \quad \bar{U}_2^1 \quad \bar{U}_3^1} \begin{bmatrix} 1 \cdots 0 \\ \vdots \quad 0 \quad \vdots \\ 0 \cdots 0 \end{bmatrix} \begin{bmatrix} -0.6425 & 0.5898 & -0.4892 \\ -0.6699 & -0.1222 & 0.7324 \\ 0.3722 & 0.7982 & 0.4736 \end{bmatrix}$$

$$V_{22}^{1*}V_{22}^{1} = \begin{bmatrix} 0.5872 & 0.3789 & -0.3143 \\ 0.3789 & 0.6521 & 0.2886 \\ -0.3143 & 0.2886 & 0.7606 \end{bmatrix} = \bar{U}^1\bar{\Lambda}_w^1\bar{U}^{1*}$$

$$= \underbrace{\begin{bmatrix} -0.6425 & -0.6699 & 0.3722 \\ 0.5898 & -0.1222 & 0.7982 \\ -0.4892 & 0.7324 & 0.4736 \end{bmatrix}}_{\bar{U}_1^1 \quad \bar{U}_2^1 \quad \bar{U}_3^1} \begin{bmatrix} 0 \cdots 0 \\ \vdots \quad 1 \quad \vdots \\ 0 \cdots 1 \end{bmatrix} \begin{bmatrix} -0.6425 & 0.5898 & -0.4892 \\ -0.6699 & -0.1222 & 0.7324 \\ 0.3722 & 0.7982 & 0.4736 \end{bmatrix}$$

Similarly, the second operating eigenvalue λ_2 yielded

$$V_{12}^{2*}V_{12}^{2} = \begin{bmatrix} 0.0464 & -0.1275 & 0.1673 \\ -0.1275 & 0.3502 & -0.4597 \\ 0.1673 & -0.4597 & 0.6035 \end{bmatrix} = \bar{U}^2\bar{\Lambda}^2\bar{U}^{2*}$$

$$= \underbrace{\begin{bmatrix} -0.2154 & -0.8861 & 0.4104 \\ 0.5918 & 0.2159 & 0.7767 \\ -0.7768 & 0.4101 & 0.4779 \end{bmatrix}}_{\bar{U}_1^2 \quad \bar{U}_2^2 \quad \bar{U}_3^2} \begin{bmatrix} 1 & \cdots & 0 \\ \vdots & 0.0001 & \vdots \\ 0 & \cdots & 0 \end{bmatrix} \begin{bmatrix} -0.2154 & 0.5918 & -0.7768 \\ -0.8861 & 0.2159 & 0.4101 \\ 0.4104 & 0.7767 & 0.4779 \end{bmatrix}$$

$$V_{22}^{2*}V_{22}^{2} = \begin{bmatrix} 0.9536 & 0.1275 & -0.1673 \\ 0.1275 & 0.6498 & 0.4597 \\ -0.1673 & 0.4597 & 0.3965 \end{bmatrix} = \bar{U}^2\bar{\Lambda}_w^2\bar{U}^{2*}$$

$$= \underbrace{\begin{bmatrix} -0.2154 & -0.8861 & 0.4104 \\ 0.5918 & 0.2159 & 0.7767 \\ -0.7768 & 0.4101 & 0.4779 \end{bmatrix}}_{\bar{U}_1^2 \quad \bar{U}_2^2 \quad \bar{U}_3^2} \begin{bmatrix} 0 & \cdots & 0 \\ \vdots & 0.9999 & \vdots \\ 0 & \cdots & 1 \end{bmatrix} \begin{bmatrix} -0.2154 & 0.5918 & -0.7768 \\ -0.8861 & 0.2159 & 0.4101 \\ 0.4104 & 0.7767 & 0.4779 \end{bmatrix}$$

Finally, the third operating eigenvalue λ_3 resulted in

$$V_{12}^{3*}V_{12}^{3} = \begin{bmatrix} 0.6929 & -0.2160 & -0.4076 \\ -0.2160 & 0.0673 & 0.1270 \\ -0.4076 & 0.1270 & 0.2399 \end{bmatrix} = \bar{U}^3\bar{\Lambda}^3\bar{U}^{3*}$$

$$= \underbrace{\begin{bmatrix} -0.8324 & 0.2253 & 0.5063 \\ 0.2594 & -0.6489 & 0.7153 \\ 0.4897 & 0.7268 & 0.4816 \end{bmatrix}}_{\bar{U}_1^3 \quad \bar{U}_2^3 \quad \bar{U}_3^3} \begin{bmatrix} 1 & \cdots & 0 \\ \vdots & 0.0001 & \vdots \\ 0 & \cdots & 0 \end{bmatrix} \begin{bmatrix} -0.8324 & 0.2594 & 0.4897 \\ 0.2253 & -0.6489 & 0.7268 \\ 0.5063 & 0.7153 & 0.4816 \end{bmatrix}$$

$$V_{22}^{3*}V_{22}^{3} = \begin{bmatrix} 0.3071 & 0.2160 & 0.4076 \\ 0.2160 & 0.9327 & -0.1270 \\ 0.4076 & -0.1270 & 0.7601 \end{bmatrix} = \bar{U}^{3}\bar{\Lambda}_{w}^{3}\bar{U}^{3*}$$

$$= \underbrace{\begin{bmatrix} -0.8324 & 0.2253 & 0.5063 \\ 0.2594 & -0.6489 & 0.7153 \\ 0.4897 & 0.7268 & 0.4816 \end{bmatrix}}_{\bar{U}_1^3 \quad \bar{U}_2^3 \quad \bar{U}_3^3} \begin{bmatrix} 0 & \cdots & 0 \\ \vdots & 0.9999 & \vdots \\ 0 & \cdots & 1 \end{bmatrix} \begin{bmatrix} -0.8324 & 0.2594 & 0.4897 \\ 0.2253 & -0.6489 & 0.7268 \\ 0.5063 & 0.7153 & 0.4816 \end{bmatrix}$$

The coefficient vectors $r^1 = \bar{U}_2^1$, $r^2 = \bar{U}_3^2$, and $r^3 = \bar{U}_3^3$ provided the most desirable vibration suppression that shows a short settling time and very small overshoot. It implied that

$$V_{22}^{1}r^{1} = V_{22}^{1}\bar{U}_2^{1} = \begin{bmatrix} 0.5876 & 0.3789 & -0.3148 \\ 0.3786 & 0.6521 & 0.2890 \\ -0.3140 & 0.2886 & 0.7602 \end{bmatrix} \underbrace{\begin{bmatrix} -0.6699 \\ -0.1222 \\ 0.7324 \end{bmatrix}}_{\bar{U}_2^1} = \begin{bmatrix} -0.6705 \\ -0.1216 \\ 0.7318 \end{bmatrix}$$

$$V_{22}^{2}r^{2} = V_{22}^{2}\bar{U}_1^{2} = \begin{bmatrix} 0.9524 & 0.1275 & -0.1669 \\ 0.1306 & 0.6497 & 0.4587 \\ -0.1714 & 0.4598 & 0.3978 \end{bmatrix} \underbrace{\begin{bmatrix} 0.4104 \\ 0.7767 \\ 0.4779 \end{bmatrix}}_{\bar{U}_3^2} = \begin{bmatrix} -0.4101 \\ -0.7774 \\ -0.4769 \end{bmatrix}$$

$$V_{22}^{3}r^{3} = V_{22}^{3}\bar{U}_1^{3} = \begin{bmatrix} 0.3085 & 0.2142 & 0.4110 \\ 0.2155 & 0.9332 & -0.1281 \\ 0.4068 & -0.1260 & 0.7582 \end{bmatrix} \underbrace{\begin{bmatrix} 0.5063 \\ 0.7153 \\ 0.4816 \end{bmatrix}}_{\bar{U}_3^3} = \begin{bmatrix} -0.5073 \\ -0.7150 \\ -0.4810 \end{bmatrix}$$

W in Eq. (5.22) was determined by combining $V_{22}^{1}r^{1}$, $V_{22}^{2}r^{2}$ and $V_{22}^{3}r^{3}$;

$$W = \begin{bmatrix} -0.6705 & -0.4101 & -0.5073 \\ -0.1216 & -0.7774 & -0.7150 \\ 0.7318 & -0.4769 & -0.4810 \end{bmatrix}$$

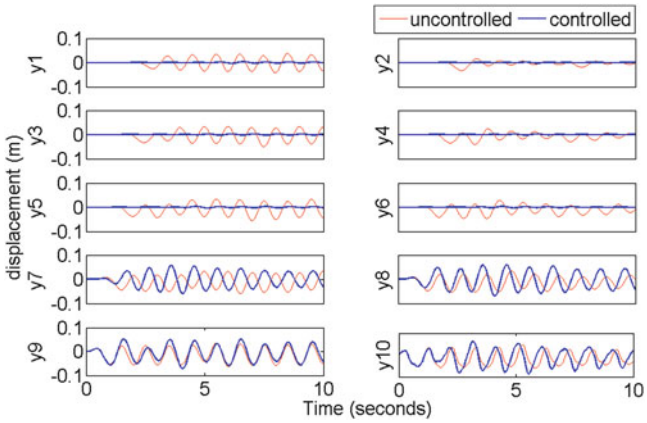

Fig. 5.3 Displacement of masses due to a chirp input at m_{10}

The real gain matrix was obtained as

$$K = W(CV)^{-1} = 1.0 \times 10^3 \begin{bmatrix} -2.6766 & -1.7254 & -0.2792 \\ 3.3596 & -3.0603 & 0.4400 \\ 1.5346 & -2.0474 & -1.7616 \end{bmatrix}$$

Figure 5.3 showed the displacement y_{1-10} of masses m_{1-10} due to the short duration chirp disturbance at m_{10}. It shows that the vibration in the isolated region that includes m_{1-6} was significantly reduced. The transient region that consists of m_{5-7} was located between the isolated and confined region and the masses that were connected to the control actuators. Both isolation and confinement of the vibration could be seen on those masses.

The vibration of m_6 was reduced while the vibrations of m_{7-8} were increased slightly. The vibrational energy was confined to m_{9-10}; therefore, masses in the confined region had higher amplitudes of vibration.

Figure 5.4 shows the actuation force for the three actuators. The maximum force at the outer actuator was greater than the other actuators and was 243.64 N. The maximum actuation forces at the inner and middle actuators were 126.54 and 148.18 N, respectively.

Based on Eq. (5.23), failure of any of the actuators was similar to setting rows of the gain matrix to zero. For example, if we assumed the outer actuator had failed, we might set the third row of the control gain matrix to zero. It implied that the third row of W was all zero, since $(CV)^{-1}$ could not have zero rows in general. The intention was to show how setting rows of W to zero after defining the control gain matrix makes a closed-loop system where its eigenvectors still belonged to the achievable eigenvectors set.

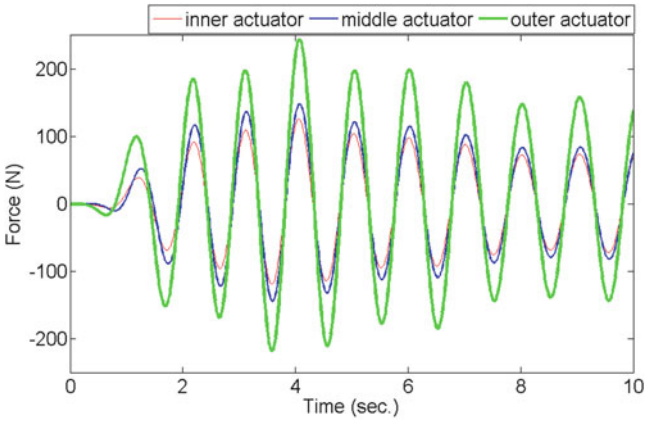

Fig. 5.4 Actuation forces due to a chirp input at m_{10}

OEC regenerated the open-loop system using the eigenvectors associated with zero eigenvalues of $V_{22}^{i\,*} V_{22}^{i}$. For example, for the first operating eigenvalue, we had

$$[V_{22}^{1}]\bar{U}_1^1 = \bar{\lambda}^1 \bar{U}_1^1$$

$$= \begin{bmatrix} 0.5876 & 0.3789 & -0.3148 \\ 0.3786 & 0.6521 & 0.2890 \\ -0.3140 & 0.2886 & 0.7602 \end{bmatrix} \begin{bmatrix} -0.6425 \\ 0.5898 \\ -0.4892 \end{bmatrix} = (0) \begin{bmatrix} -0.6425 \\ 0.5898 \\ -0.4892 \end{bmatrix} = \begin{bmatrix} 0 \\ 0 \\ 0 \end{bmatrix}$$

If the outer actuator was assumed to have failed, the third row of the $[V_{22}^{1}]$ was set to zero and the new matrix was called $[\tilde{V}_{22}^{1}]$.

$$[\tilde{V}_{22}^{1}]^{*}[\tilde{V}_{22}^{1}] = \tilde{U}^1 \tilde{\Lambda}^1 \tilde{U}^{1*}$$

$$= \begin{bmatrix} 0.5876 & 0.3786 & 0 \\ 0.3789 & 0.6521 & 0 \\ -0.3148 & 0.2890 & 0 \end{bmatrix} \begin{bmatrix} 0.5876 & 0.3789 & -0.3148 \\ 0.3786 & 0.6521 & 0.2890 \\ 0 & 0 & 0 \end{bmatrix}$$

$$= \begin{bmatrix} 0.4886 & 0.4695 & -0.0756 \\ 0.4695 & 0.5688 & 0.0692 \\ -0.0756 & 0.0692 & 0.1827 \end{bmatrix}$$

$$= \begin{bmatrix} -0.6764 & 0.3602 & 0.6425 \\ -0.7366 & -0.3310 & -0.5898 \\ 0.0002 & -0.8721 & 0.4892 \end{bmatrix} \begin{bmatrix} 1 & 0 & 0 \\ 0 & 0.24 & 0 \\ 0 & 0 & 0 \end{bmatrix} \begin{bmatrix} -0.6764 & -0.7366 & 0.0002 \\ 0.3602 & -0.3310 & -0.8721 \\ 0.6425 & -0.5898 & 0.4892 \end{bmatrix}$$

The open-loop system could be regenerated again, since the eigenvectors associated with zero eigenvalue of ${V_{22}^i}^* V_{22}^i$ and ${\tilde{V}_{22}^i}^* \tilde{V}_{22}^i$ were identical.

$$
\begin{aligned}
&[\widehat{V}_{22}^{1}]\widehat{U}^{1} = \widehat{\lambda}^{1}\widehat{U}^{1} \\
&= \begin{bmatrix} 0.5876 & 0.3789 & -0.3148 \\ 0.3786 & 0.6521 & 0.2890 \\ 0 & 0 & 0 \end{bmatrix} \begin{bmatrix} -0.6425 \\ 0.5898 \\ -0.4892 \end{bmatrix} = (0) \begin{bmatrix} -0.6425 \\ 0.5898 \\ -0.4892 \end{bmatrix} = \begin{bmatrix} 0 \\ 0 \\ 0 \end{bmatrix}
\end{aligned}
$$

Previously, we had

$$
[V_{22}^{1}]\widehat{U}^{1} = \begin{bmatrix} 0.5876 & 0.3789 & -0.3148 \\ 0.3786 & 0.6521 & 0.2890 \\ -0.3140 & 0.2886 & 0.7602 \end{bmatrix} \begin{bmatrix} -0.6425 \\ 0.5898 \\ -0.4892 \end{bmatrix} = \begin{bmatrix} 0 \\ 0 \\ 0 \end{bmatrix}
$$

It was seen that both V_{22}^{1} and $\widehat{V}_{22}^{1}$ could regenerate the open-loop eigenvector using the eigenvector associated with zero eigenvalue of ${V_{22}^i}^* V_{22}^i$ and ${\widehat{V}_{22}^i}^* \widehat{V}_{22}^i$, respectively. Similar results for the second and the third operating eigenvalues could be found. It implied that the system with the failed actuator was still using the coefficient vectors that generated the closed-loop eigenvectors orthogonal to the open-loop eigenvectors.

The control gain matrix for the system with the failed actuator was

$$
K = 1.0 \times 10^3 \begin{bmatrix} -1.3211 & -0.8670 & -0.1340 \\ 1.5735 & -1.5267 & 0.1759 \\ 0 & 0 & 0 \end{bmatrix}
$$

Figure 5.5 shows the displacements of masses of the system due to the chirp disturbance to m_{10}. Similar to the system with working actuators stated earlier, a good isolation could be seen at m_{1-6}. Behaviors of the masses in transient and confined regions were similar to the system with working actuators. Figure 5.6 compares the displacements of m_1 in the complete system and the system with the failed actuator. The time histories of the displacements were slightly different. A slightly slower decay could be seen in the system with the failed actuator. Actuation forces of the actuators were shown on Fig. 5.7. Maximum actuation forces of the inner and middle actuators were 132.18 N and 150.94 N, respectively. The amount of increase in the actuation forces of the inner and middle actuators were 5.62 N and 2.76 N, respectively.

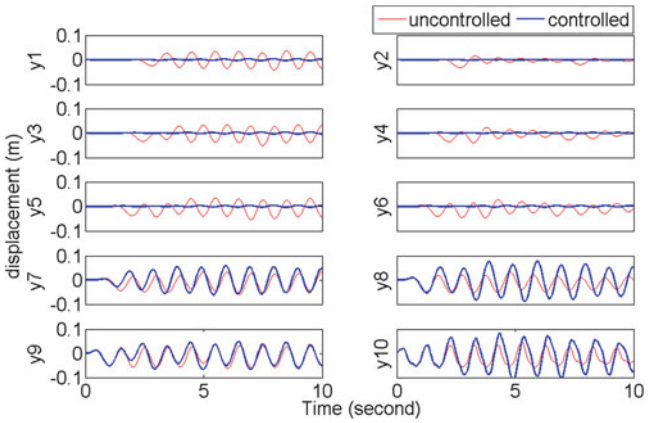

Fig. 5.5 Comparison of displacement of masses due to a unit impulse at m_{10}, using reduced gain matrix for the case with three sensors and two actuators

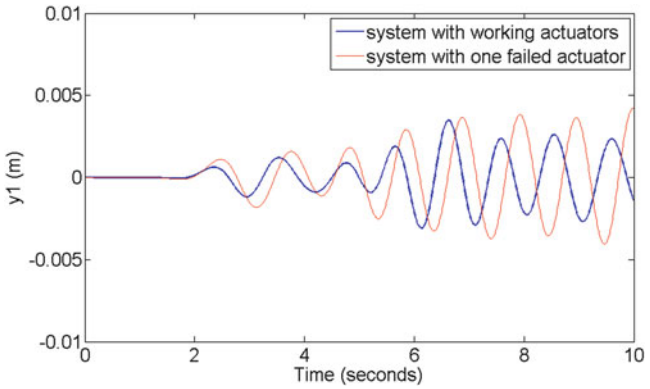

Fig. 5.6 Comparison of displacement of m_1 in the system of lumped masses with working actuators to the system with one failed actuator due to a chirp disturbance at m_{10}

5.4 Case Study: Isolation of Vibration in a Plate

Figure 5.8 shows the nodes of a finite element model of a plate that is simply supported at four edges with Young's modulus of 2.09×10^9 N m^{-2} and the Poisson's ratio is 0.33. It is a square plate, with length of 40 cm, and thickness of 1 mm. A code was written in Matlab for modeling the plate and solving its equation of motion. Mindlin plate theory was used to define the displacement field of the plate; therefore, there were 3 degrees of freedom for each node. Two of the degrees of freedom were in-plane displacements (u and v directions) and the third one was the transverse displacement y. Using linear quadrilateral elements, we used the procedure reported in [27] for calculating the mass and stiffness matrices of each

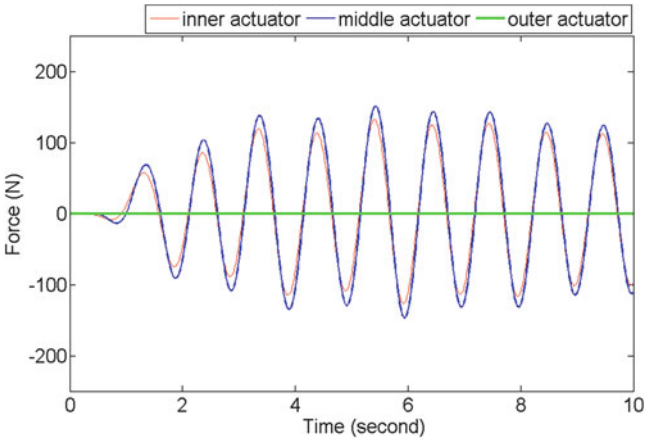

Fig. 5.7 Actuation forces for the system with failed actuator

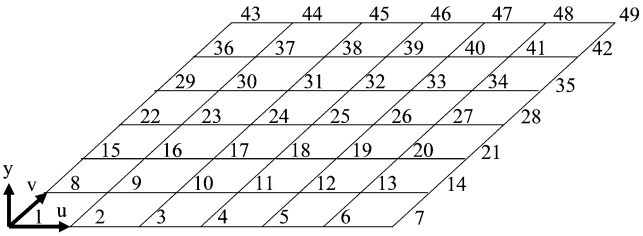

Fig. 5.8 Simply supported plate with 49 nodes and 36 elements

element. The dimensions of global mass and stiffness matrices, were 149×149, since the model had 49 nodes and each had 3 degrees of freedom. Damping matrix D_d, was assumed to be a linear damping defined as $D_d = 0.2M + 0.002K_s$ after scaling the mass and stiffness matrices. As a result, the dimension of the state matrix A for the state space realization of system in Eq. (5.1) was 298×298.

The disturbance force applied to the plate was a sine wave with a frequency of 2 kHz and amplitude of 10 N. The disturbance force was applied to the plate at node 27 and was normal to the plate that results in the plate bending.

We consider five cases with different scenarios for the actuators. Case 1 was a plate with three working actuators, case 2 was similar to case 1 with the middle actuator failed. Case 3 was similar to case 1 with a failed outer actuator. The control gains for cases 4 and 5 were designed specifically for two actuators. Case 4 was a plate with two control actuator at the nodes where working actuators of case 2 are located. Case 5 also had two actuators at the location of the working actuators of case 3.

As stated earlier, the operating eigenvalues were the greatest open-loop eigenvalues of the system, for all the cases the operating eigenvalues were $-24.9799 + 155.743\text{i}$, $-24.9799 + 155.743\text{i}$, and $-24.8108 + 155.2264\text{i}$. Since

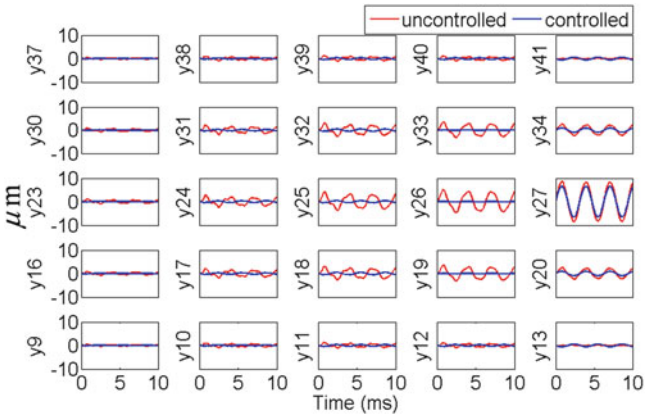

Fig. 5.9 Case 1, displacements of the nodes of plate due to a 2 kHz sine wave disturbance at node 27. Actuators are on nodes 19, 26, and 33

using complex conjugates of the operating eigenvalues results in similar closed-loop systems, we only used the operating eigenvalues with positive imaginary parts.

We assumed that there were sensors collocated with the actuators and the signals from those sensors were used for position feedback. As explained earlier, there were 26 possible closed-loop systems for the systems in cases 1, 2, and 3 with three actuators and there were three possible closed-loop systems for systems of cases 4 and 5 where two actuators were used.

5.4.1 Case 1: Plate with Three Working Actuators

As shown in earlier studies [21], when the greatest open-loop eigenvalues were chosen as the operating eigenvalues, all the closed-loop systems would be identical. Also, all the off-diagonal elements were small in comparison to diagonal elements, and the control becomes decoupled. In this case the control gain matrices were converged to the following matrix.

$$K = 1.0 \times 10^4 \begin{bmatrix} -2.1656 & 0.0420 & 0.0267 \\ 0.0034 & -2.1985 & 0.0030 \\ -0.0319 & -0.0444 & -2.2220 \end{bmatrix}$$

In fact, setting the off-diagonal elements did not change the results noticeably. Figure 5.9 shows that the suppression of vibrations on different nodes of the plate. Actuation forces also can be seen on Fig. 5.10. The maximum actuation forces were 0.86 N on nodes 19, 6.60 N on node 26, and 0.86 N on node 33. Because of the symmetry, the actuation forces of the actuators on nodes 19 and 33 were coincident.

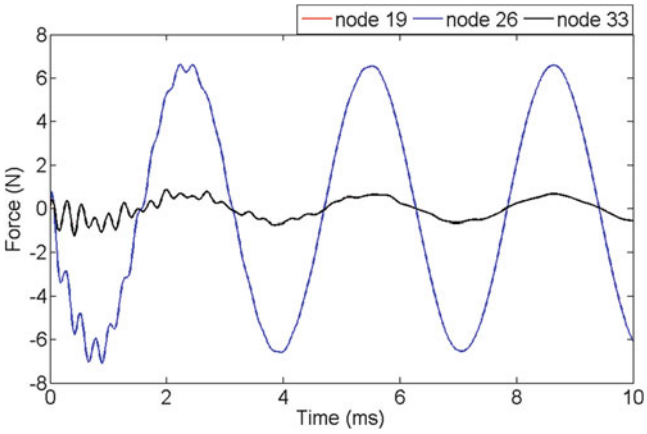

Fig. 5.10 Case 1, actuation forces at nodes 19 and 33 are identical. The amplitude of the disturbance is 10 N

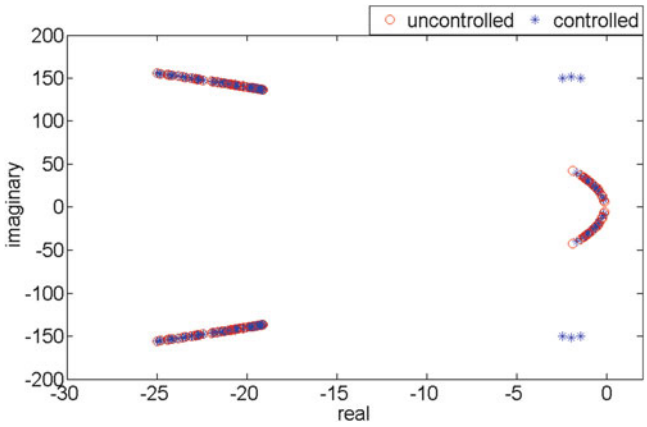

Fig. 5.11 Case 1, eigenvalues of the open-loop and closed-loop systems

Figure 5.11 illustrates the distributions of the open-loop and closed-loop poles. It was seen that three pairs of the closed-loop poles were moved away from the locus of the open-loop poles.

5.4.2 Case 2: Plate with Two Working Actuators and Failed Middle Actuator

We assumed that the middle actuator located on node 33 had failed. This resulted in setting the middle row of the control gain matrix to zero. Figure 5.12 shows

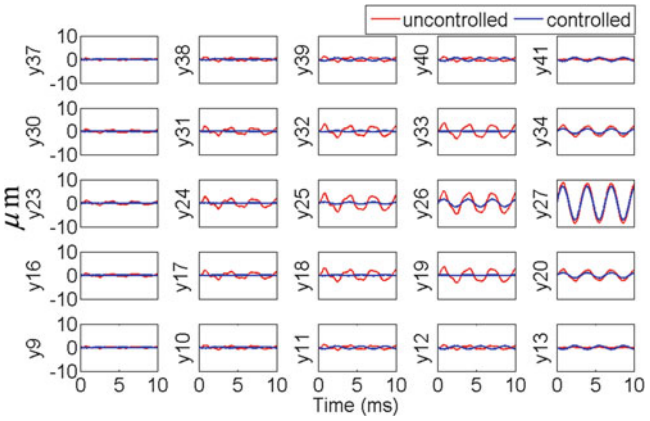

Fig. 5.12 Case 2, displacements of the nodes of plate due to a 2 kHz sine wave disturbance at node 27. Working actuators on nodes 19, 26, and failed actuator on node 33

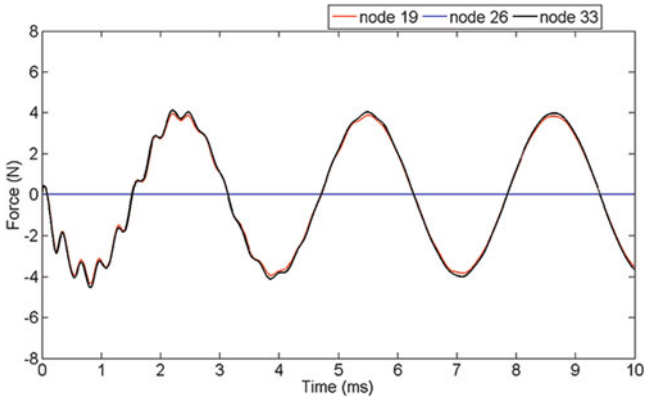

Fig. 5.13 Case 2, actuation forces. The amplitude of the disturbance is 10 N

the displacement of the nodes of the plate. The noticeable difference was the displacement of node 26, which has a failed actuator. Maximum actuation forces were shown on Fig. 5.13. The middle actuator had not applied any force to the system. The maximum actuation force on the actuator on node 19 was 3.94 N and on the node 33 was 4.12 N. The actuation forces are increased in comparison to case 1. The slight difference was because the control gain matrix is not symmetric. The control gain matrix was

$$K = 1.0 \times 10^4 \begin{bmatrix} -2.1656 & 0.0420 & 0.0267 \\ 0 & 0 & 0 \\ -0.0319 & -0.0444 & -2.2220 \end{bmatrix}$$

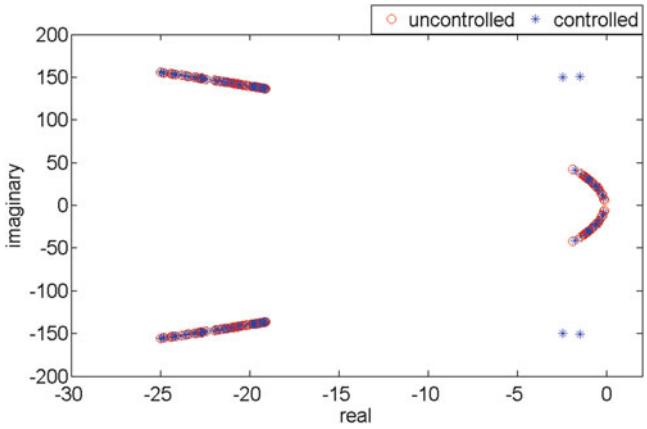

Fig. 5.14 Case 2, eigenvalues of the open-loop and closed-loop systems

Figure 5.14 shows the closed-loop and open-loop poles of the system. It was seen that two closed-loop poles were moved away from the open-loop poles cluster, as was expected since there were two working actuators. Comparing Figs. 5.14 and 5.11, one finds that the moved closed-loop poles were placed in a similar region.

5.4.3 Case 3: Plate with Two Working Actuators and Failed Outer Actuator

In this case, we assume that the faulty actuator was located on node 33. Therefore the control gain matrix was

$$K = 1.0 \times 10^4 \begin{bmatrix} -2.1656 & 0.0420 & 0.0267 \\ 0.0034 & -2.1985 & 0.0030 \\ 0 & 0 & 0 \end{bmatrix}$$

The displacement shown on Fig. 5.15 shows a good isolation on different nodes of the plate. The displacement of the node 25; however, was different form case 1, because of the failed actuator. Time history of the actuation forces was shown in Fig. 5.16. The maximum actuation force of the actuator on node 19 is 0.72 N and on node 26 is 7.2 N which was very close to the actuation forces in case 1.

Figure 5.17 shows the displacement of the middle node of the plate for cases 1, 2, and 3. The amplitudes of vibration for all the cases were very close. Vibration in Case 3 was in phase with the displacement in case 1. In case 2, however, there was a $\pi/2$ phase shift with respect to the response of case 1. This showed a great

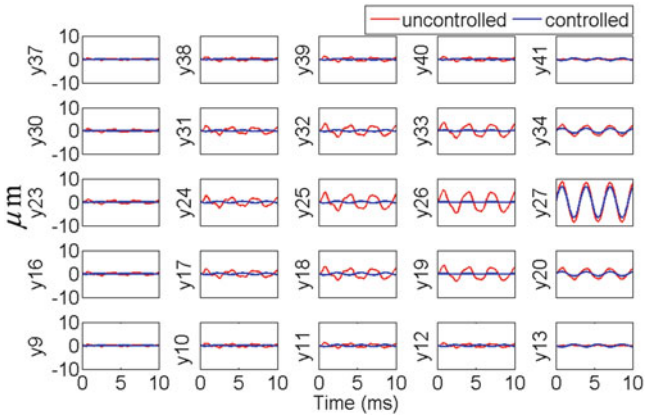

Fig. 5.15 Case 3, displacements of the nodes of plate due to a 2 kHz sine wave disturbance at node 27. Working actuators on nodes 19, 33, and failed actuator on node 26

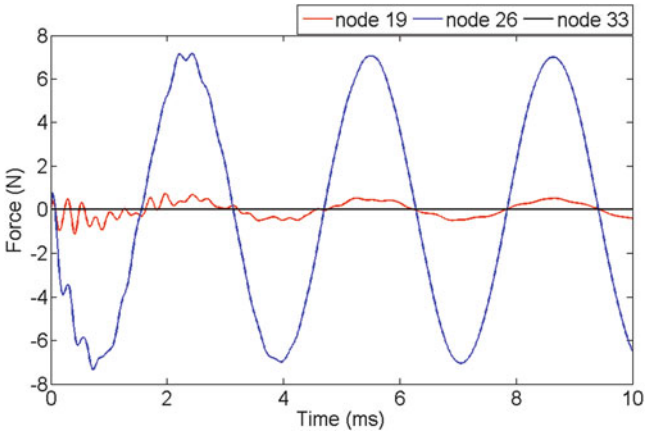

Fig. 5.16 Case 3, actuation forces. The amplitude of the disturbance is 10 N

robustness for the OEC to the actuator failure since that failure of each of the actuators had a local effect in the vicinity of the failed actuator, but the overall vibration cancelation in the plate had remained significantly intact. Figure 5.18 shows the closed-loop and open-loop poles of the system that indicates two of the closed-loop poles were moved away from the open-loop poles cluster similar to cases 1 and 2.

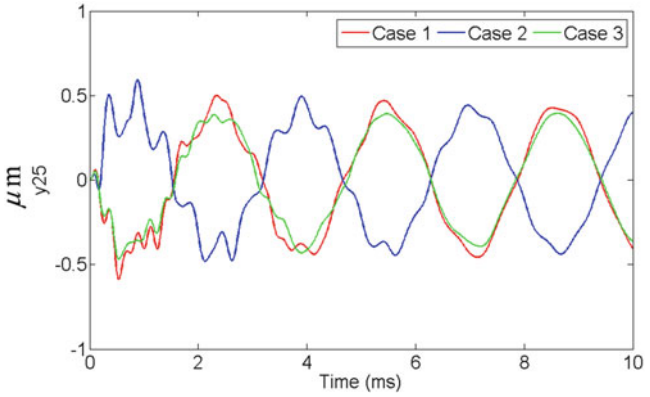

Fig. 5.17 Displacement of plate's middle node for cases 1, 2, and 3

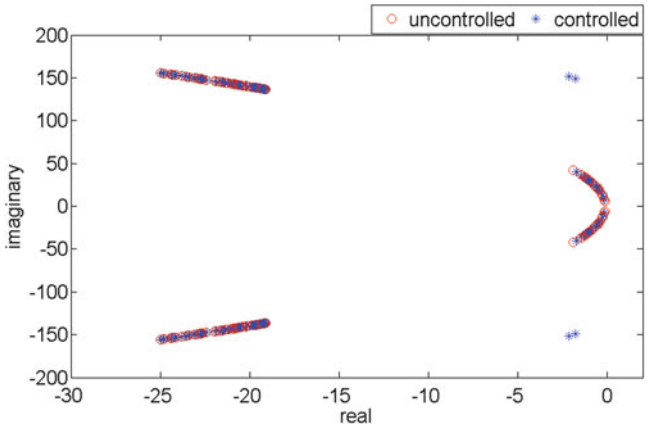

Fig. 5.18 Case 3, eigenvalues of the open-loop and closed-loop systems

5.4.4 Case 4: Plate with Two Working Actuators Similar to Case 2

Case 4 was the control of the vibration in a plate with two working actuators on nodes 19 and 33. It was similar to case 2 unless there was no failed actuator and the control gain matrix was

$$K = 1.0 \times 10^4 \begin{bmatrix} -2.2027 & 0.0028 \\ 0.0028 & -2.2027 \end{bmatrix}$$

that was symmetric due to the symmetry of the geometrical symmetry of plate and the location of the actuators and disturbance. The same property in the gain

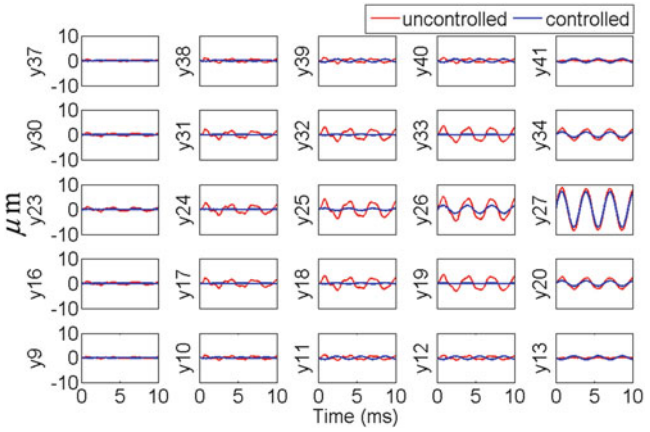

Fig. 5.19 Case 4, displacements of the nodes of plate due to a 2 kHz sine wave disturbance on node 27, actuators are on nodes 19 and 26

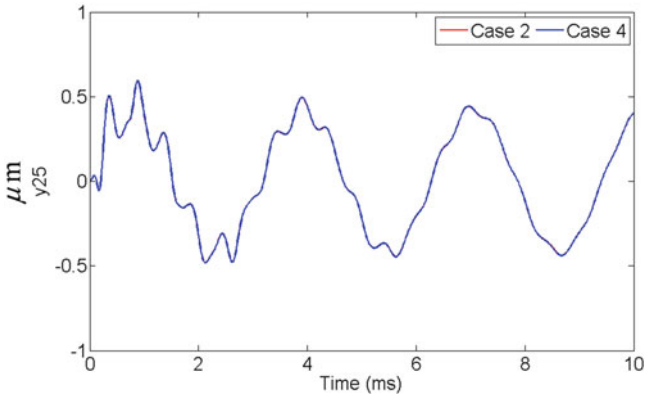

Fig. 5.20 Identical displacements of plate's middle node for cases 2 and 4

matrix of the case 1 could be seen here. The off-diagonal elements were three orders of magnitudes smaller than the diagonal elements; therefore, a decoupled control could be expected. Figure 5.19 shows the displacements of different nodes on the plate depicting a good isolation throughout the plate similar to earlier cases. A comparison between the displacements of node 25, the middle point in the plate, is shown in Fig. 5.20. It was seen that the displacements are identical. The time history of the actuation forces was shown in Fig. 5.21. The maximum force at the actuators on nodes 19 and 33 were identically 4.03 N, which was close to the actuation forces in case 2. The distribution of the eigenvalues of the open-loop and closed-loop systems was shown in Fig. 5.22. Two of the closed-loop system eigenvalues, similar to those in case 2, were moved away from the cluster of the open-loop eigenvalues.

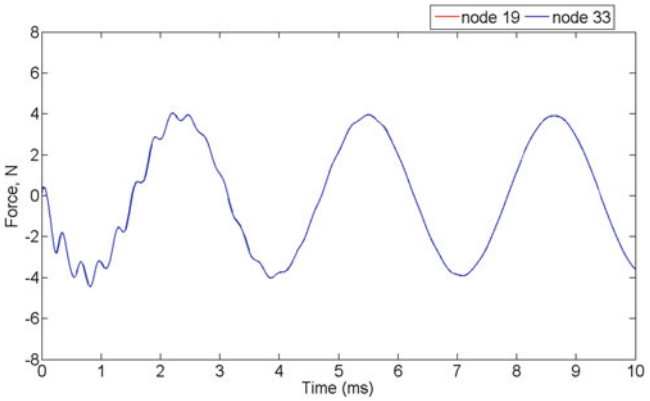

Fig. 5.21 Case 4, actuation forces in actuators on nodes 19 and 33 are identical. The amplitude of the disturbance is 10 N

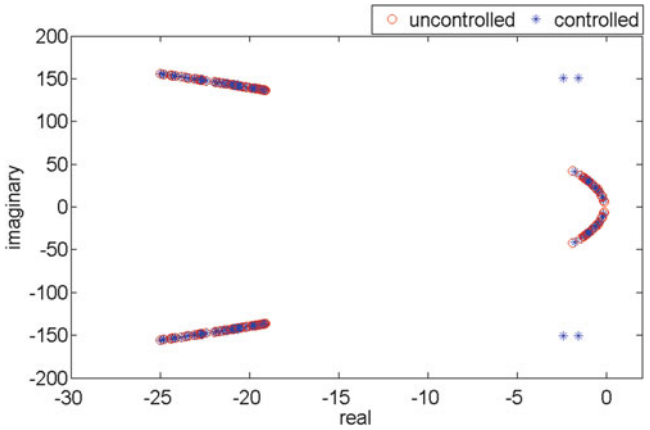

Fig. 5.22 Case 4, eigenvalues of the open-loop and closed-loop systems

5.4.5 Case 5: Plate with Two Working Actuators Similar to Case 3

Case 5 investigated the vibration isolation of the plate using two actuators, which were placed on nodes 19 and 26, the same locations as the working actuators of the case 3. The control gain matrix was

$$K = 1.0 \times 10^4 \begin{bmatrix} -2.2027 & -0.0032 \\ -0.0026 & -2.2064 \end{bmatrix}$$

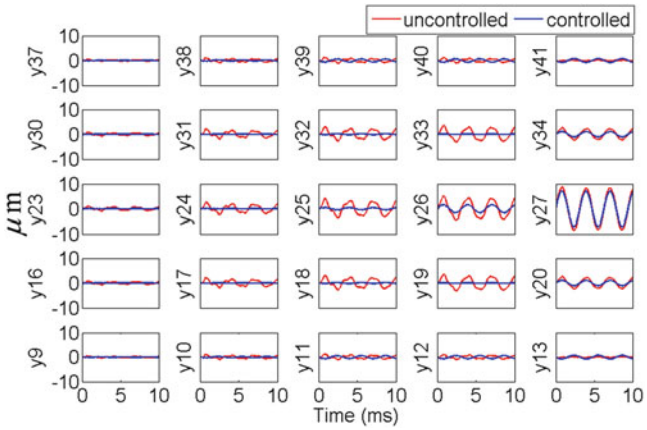

Fig. 5.23 Case 5, displacements of the nodes of plate due to a 2 kHz sine wave disturbance on node 27, actuators are on nodes 19 and 26

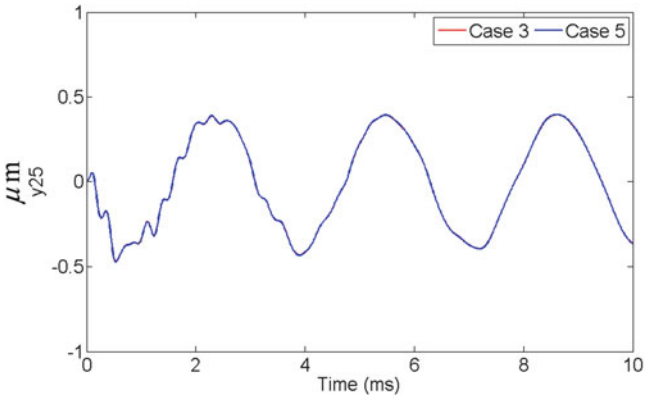

Fig. 5.24 Identical displacement of the plate's middle node for cases 3 and 5

similar to case 4. Figure 5.23 shows vibration similar to the earlier cases. The identical behavior of the middle point of the plate in case 3 and 5 was depicted in Fig. 5.24. Also, the time histories of the actuation forces were shown in Fig. 5.25. The Maximum actuation forces of the actuators on nodes 19 and 26 were 0.73 N and 7.16 N, respectively, which was very close to case 3. Similar to earlier cases, two of the closed-loop eigenvalues were moved away from the open-loop cluster, as shown in Fig. 5.26.

Comparing the results of the case 2 and 3 to case 1, one could see a reliable control design when OEC was used. The actuation forces in working actuators in cases 2 and 3 that contain failed actuators were very close to the forces of the system with three working actuators. Similar displacement time history could be seen

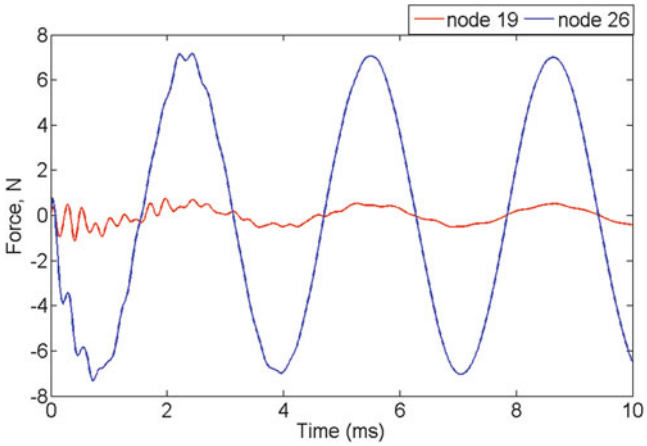

Fig. 5.25 Case 5, actuation forces. The amplitude of the disturbance is 10 N

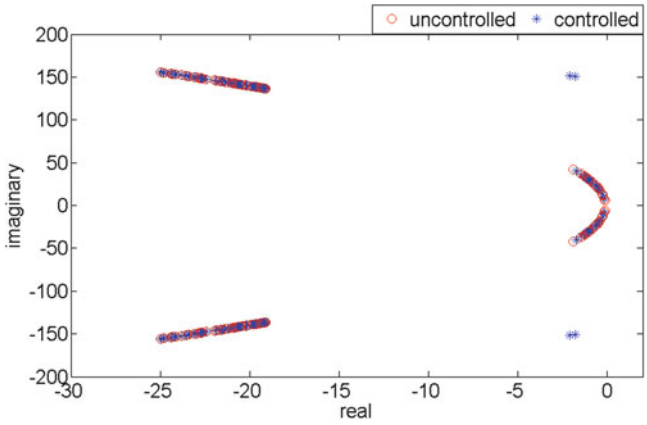

Fig. 5.26 Case 5, eigenvalues of the open-loop and closed-loop systems

throughout the plate except nodes with failed actuators. Moreover, comparing case 4 to 2 and 5 to 3, respectively, shows that there was slight difference between the system with one failed actuator and the system that was designed for two actuators. Orthogonal eigenstructure control with three actuators proved to be robust in such a way that the behavior of the system with one failed and two working actuators were identical to the behavior of the system that was designed primarily for two actuators. Table 5.1 shows the closed-loop eigenvalues that were moved away from the locus of the open-loop eigenvalues. It shows that for all the cases, the poles were placed in a small region. The rest of the closed-loop eigenvalues were moved slightly on the locus of the open-loop poles, without noticeable deviation away from the cluster.

Table 5.1 Moved closed-loop poles in cases 1–5

	Pair 1	Pair 2	Pair 3
Case 1	$-1.99 \pm 151.35i$	$-1.43 \pm 150.17i$	$-2.47 \pm 150.08i$
Case 2	$-1.50 \pm 150.79i$	$-2.46 \pm 150.13i$	
Case 3	$-1.78 \pm 148.91i$	$-2.11 \pm 151.25i$	
Case 4	$-1.56 \pm 150.95i$	$-2.40 \pm 150.60i$	
Case 5	$-1.78 \pm 150.54i$	$-2.11 \pm 151.19i$	

5.5 Applicability of OEC

Proper use of design freedom is depended on the experience of the controller designer. The improper use of the design freedom may cause excessive actuation forces. OEC reduces those design freedoms that are depended on the designer experience. It limits the design freedom to vectors orthogonal to the eigenvectors of the system and allows the controller designer to substitute the eigenvectors with vectors that are almost orthogonal to them. OEC can systematically determine the feedback control law with minimal input from a controller designer and is capable of performing robustly in the presence of a wide variety of disturbances.

OEC eliminates the need for defining the desirable eigenvectors and eigenvalues of the closed-loop system, which are usually needed by other eigenstructure assignment methods. This significantly reduces the amount of time needed for developing a new controller for structural control. Orthogonal eigenstructure control is able to suggest a set of closed-loop systems. OEC reduces the controller development cycle significantly through a mathematically sound approach that can easily be implemented to a broad range of systems in practice.

For the cases studies presented in this chapter, the control gains determined by OEC were almost diagonal that suggests a decoupled control. Therefore the effects of the failure of an actuator on the performance of the system will be limited. This makes OEC more readily applicable to real-life applications, by better dealing with limitations that happen in case of components failure.

5.6 Conclusion

The robustness of the OEC to the actuator failure in vibration cancelation in a plate was studied in this chapter. First, a simple system of lumped masses was considered and the effect of failure of an actuator was explained. Then, the same method was used to describe the effect of the failed actuator in a plate. Finite element analysis was used to model the plate and the plate response to force perturbations was simulated. Five cases were considered for the different scenarios with the actuators of the plate and the results were compared. It was shown that when the operating eigenvalues were the farthest open-loop eigenvalues from

the origin, a reliable and almost decoupled control could be achieved. Behaviors of the systems with failed actuators followed closely the behavior of the system with no faulty actuators. Moreover, the cancelations of vibration in the systems with failed actuators were almost identical to the systems that were primarily designed for two actuators. While there was no need to define the required locations for the closed-loop poles, few pairs of the closed-loop eigenvalues were moved away from the locus of the open-loop eigenvalues. The number of pairs of the moved eigenvalues was equal to the number of the actuators in each case. Since in all the cases the closed-loop eigenvalues were moved to one specific area, the behaviors of all the systems were similar and the control was robust to the actuator failure.

Key Symbols

A	Open-loop state matrix
A_c	Closed-loop state matrix
B	Input matrix
C	Output matrix
E	Disturbance input matrix
E_i	Modal energy of ith mode
f	Disturbance
I	Identity matrix
K	Gain matrix
m	Number of inputs (actuators/sensors)
N^i	Matrix that spans the null space of ith mode
n	Dimension of second order system
r^i	Vector of coefficients
$S_{\lambda i}$	Augmented matrix associated with λ_i
u	Input vector
U_i	Left unitary matrix of $S_{\lambda i}$
$\bar{U}^i$	Eigenvalue matrix of $V_{12}^{i*}V_{12}^i$ and $V_{22}^{i*}V_{22}^i$
$\bar{U}_w^i$	Eigenvalue matrix of $V_{22}^{i*}V_{22}^i$, equals to $\bar{U}^i$
$\bar{U}_j^i$	Eigenvalue of $V_{12}^{i*}V_{12}^i$ associated with non-unity eigenvalues
$\bar{U}_J^i$	Eigenvalue of $V_{12}^{i*}V_{12}^i$ associated with unity eigenvalue
V_i	Right unitary matrix of $S_{\lambda i}$
V_{12}^i	Upper part of N^i
V_{22}^i	Lower part of N^i
V	Appended matrix of $[V_{12}^i]r^i$
W	Appended matrix of $[V_{22}^i]r^i$
x	State vector
$\dot{x}$	Time derivative of state vector
y	Output vector
ϕ_i	ith closed-loop eigenvalue

ϕ_i^a Achievable eigenvector of ith mode
λ_i ith operating eigenvalue
$\bar{\lambda}_j^i$ Eigenvalues of $V_{12}^{i*}V_{12}^i$
$\bar{\Lambda}_i$ Eigenvalue matrix of $V_{12}^{i*}V_{12}^i$
$\bar{\Lambda}_w^i$ Eigenvalue matrix of $V_{22}^{i*}V_{22}^i$
Σ_i Matrix of singular values of $S_{\lambda i}$
$*$ Conjugate transpose symbol

References

1. D'Azzo JJ, Houpis CH (1995) Linear control system analysis and design: conventional and modern, 4th edn. McGraw-Hill
2. Moore BC (1976) On the flexibility offered by state feedback in multivariable systems beyond closed loop eigenvalue assignment. IEEE Trans Autom Control 21:689–692
3. Tao G, Ma X, Joshi SM (2000) Adaptive state feedback control of systems with actuator failures. In: American control conference, Chicago, IL
4. Tao G, Joshi SM, Ma X (2001) Adaptive state feedback and tracking control of systems with actuator failures. IEEE Trans Autom Control 46(1):78–95
5. Tao G, Chen S, Joshi SM (2002) An adaptive control scheme for systems with unknown actuator failures. Automatica 38:1027–1034
6. Tang X, Tao G, Joshi SM (2007) Adaptive actuator failure compensation for nonlinear mimo systems with an aircraft control application. Automatica 43:1869–1883
7. Fei J et al (2005) Robust adaptive control scheme for discrete-time system with actuator failures. J Dyn Syst Meas Control 127:520–526
8. Chen W, Saif M (2005) An actuator fault isolation strategy for linear and nonlinear systems. In: American control conference, Portland, OR
9. Chen W, Jiang J (2005) Fault-tolerant control against stuck actuator faults. IEE Proc Control Theory Appl 152(2):138–146
10. Yang Y, Yang GH, Soh YC (2000) Reliable control of discrete-time systems with actuator failure. IEE Proc Control Theory Appl 147(4):428–432
11. Seo CJ, Kim BK (1996) Robust and reliable Hoo control for linear systems parameter uncertainty and actuator failure. Automatica 32(3):465–467
12. Wang R, Liu M, Zhao J (2007) Reliable H_{oo} control for a class of switched nonlinear systems with actuator failures. Nonlinear Anal Hybrid Syst 1:317–325
13. Zhao Q, Cheng C (2003) Robust state feedback for actuator failure accommodation. In: The American control conference, Denver, CO
14. Liu GP, Patton RJ (1998) Robust eigenstructure assignment combining time- and frequency-domain performance specifications. Int J Robust Nonlinear Control 8:61–78
15. Wang G, Liang B, Duan G (2005) Reconfiguring second-order dynamic systems via P-D feedback eigenstructure assignment: a parametric method. Int J Control Autom Syst 3(1):109–116
16. Zhang Y, Jiang J (2001) Integrated active fault-tolerant control using IMM approach. IEEE Trans Aerosp Electron Syst 37(4):1221–1235
17. Jiang J (1994) Design of reconfigurable control systems using eigenstructure assignments. Int J Control 59(2):395–410
18. Apkarian P, Tuan HD, Bernussou J (2000) Analysis, eigenstructure assignment and H2 multi-channel synthesis with enhanced LMI characterizations. In: Proceedings of the 39th IEEE conference on decision and control Sydney, Sydney, Australia
19. Rastgaar M, Ahmadian M, Southward SC (2010) Orthogonal eigenstructure control for vibration suppression. J Vib Acoust 132(1):1–10

20. Rastgaar MA, Ahmadian M, Southward SC (2009) Orthogonal eigenstructure control with non-collocated actuators and sensors. J Vib Control 15(7):1019–1047
21. Rastgaar M, Ahmadian M, Southward SC (2010) Vibration cancellation in a plate using orthogonal eigenstructure control. ASME J Appl Mech 77:061007
22. Rastgaar M, Ahmadian M, Southward SC (2010) Experimental application of orthogonal eigenstructure control for structural vibration cancellation. J Sound Vib 329(19):3873–3887
23. Rastgaar MA, Ahmadian M, Southward SC (2009) A review on eigenstructure assignment methods and orthogonal eigenstructure control of structural vibrations. Shock Vib 16(5):555–564
24. Rastgaar M, Ahmadian M, Southward SC (2007) Vibration confinement by minimum modal energy eigenstructure assignment. In: ASME international design engineering technical conferences, IDETC/CIE 2007, Las Vegas, NV
25. Shelley FJ, Clark WW (2000) Experimental application of feedback control to localize vibration. J Vib Acoust 122:143–150
26. Rastgaar M, Ahmadian M, Southward SC (2007) Effect of the actuators' location on vibration confinement using minimum modal energy eigenstructure assignment. In: ASME international design engineering technical conferences, IDETC/CIE 2007, Las Vegas, NV
27. Weaver W, Johnston PR (1987) Structural dynamics by finite element. Prentice-Hall